Soft Computing (2024) 28:4489–4501
https://doi.org/10.1007/s00500-023-08837-y

APPLICATION OF SOFT COMPUTING

Method for automatic detection of movement-related EEG pattern time boundaries

I. V. Shcherban[1] · D. M. Lazurenko[1] · O. G. Shcherban[1] · D. G. Shaposhnikov[1] · N. E. Kirilenko[1] · A. V. Shustova[1]

Accepted: 14 June 2023 / Published online: 4 July 2023

Abstract

The study was aimed at developing a new automatic search technique for specific invariant patterns of movement-related brain potentials reflected in multidimensional electroencephalogram (EEG) signals. An adaptive band-pass filter with bandwidth closely matching the spectrum of the desired EEG pattern at the observed moment was synthesized based on the Singular Spectrum Analysis methodology. The preliminary filtering of the original EEG signals provides the required sensitivity for subsequent searching of time boundaries in patterns. The correctness of the developed method was confirmed with standard machine learning tools through the validation of the adaptive search method carried out on the general set of initial data. It is shown that the synthesized method has provided a reliable automatic search for induced pre-movement EEG patterns and the correct determination of their time boundaries (accuracy up 29% on average and reached maximum values to 100% for some individuals). The developed method expands the existing tools to improve the functionality and reliability of various Brain-computer interfaces for various purposes, including medical applications for paralyzed patients.

Keywords Electroencephalogram · Movement-related brain potentials · Initial and final time boundaries · Automatic detection · Adaptive band-pass filter · Singular spectrum analysis · Hausdorff distance · Human voluntary motor activity

1 Introduction

It is known that a noninvasive approach based on electroencephalogram (EEG) signals has proven to be very useful in Brain-computer interface (BCI). BCIs strictly do not use normal neuromuscular output pathways. The original idea of BCI is to replace or restore brain function in patients with neuromuscular disorders such as amyotrophic lateral sclerosis, stroke, and spinal cord injury (McFarland et al. 2017). The study on the features of electrophysiological indicators associated with brain potentials is a key aspect in improving the accuracy and reliability of the BCI. Usually these indicators (brain patterns) in EEG signals are random a priori undefined structures with unknown temporal dynamics and fluctuations of frequency oscillators with various intensities. Nowadays, the search in multidimensional EEG signals for these brain patterns is being thoroughly studied (Abiri et al. 2019). The widely used methods for analyzing and decoding brain EEG signals can promote widespread application of neural control. These methods have an impact on the accuracy of the pattern classification of electrical brain activity (Colamarino et al. 2018).

Nevertheless, the character of movement-related brain potential (MRP) patterns being displayed in EEG signals sets a limit on the use of a classical approaches to solving the problem of their automatic detection (Takashima et al. 2020). First and foremost, the quasistationary nature of the EEG itself makes it problematic to analyze and interpret the bioelectric activity of the brain (Craik et al. 2019). There have been numerous attempts to use spectral density decomposition method for automatic detection of specific brain patterns associated with the epileptic foci (Türk and

✉ I. V. Shcherban
ivsherban@sfedu.ru

[1] Research Center for Neurotechnology, Southern Federal University, Rostov-on-Don, Russian Federation 344006

Özerdem 2019), or to assess the effects of EEG synchronization/desynchronization (Li et al. 2019), and others. Second, the main disadvantage of known approaches, however, is the assumption that several parameters, including nonlinear indicators in different frequency regions of the signal, are known a priori. The EEG assumes the presence of a set of narrow-band MRPs that specifically reflect the voluntary motor activity of a person associated with movement preparation (Readiness potentials, RP), or movement execution (Motor potentials, MP), or motor imagery (MI) and inner speech activity (IS). Parameters of recorded MRPs depend on the nature of the activity being executed—visual or kinesthetic imagination (Lee et al. 2019). Moreover, the frequency spectrum of target MRP patterns is determined by the current psychophysiological and functional state of a person, and, for example, the type of movement being prepared—voluntary motor execution or ballistic (spontaneous) (Lazurenko et al. 2018; Chen et al. 2019). Thus, as a rule, the frequency composition and power spectrum of these specific EEG patterns are not known in advance as they are determined by a sufficiently large set of uncontrolled random factors unknown to the researcher. Another substantial problem in the study of voluntary motor activity, especially, motor imagery is the blurring of time boundaries in determining the processes of planning, preparation, and execution of motor acts (Freer and Yang 2020). This problem does not allow for a sufficiently reliable coherent summation of induced brain electrograms, as compared to evoked potentials (Jin et al. 2012; Eidel and Kübler 2020; Kübler et al. 2021). In addition, the modal frequencies of various brain rhythm oscillators usually associated with an individual's different activity can demonstrate a very high variability even during one experimental series. This phenomenon may be caused by fatigue and monotony (Sengupta 2020). Thus, several problems related to the detection, interpretation, and classification of MRPs accompanying voluntary motor activity (including motor imagery) of a person have not yet been fully resolved. Such nonstationary character of the required EEG patterns, as well as the a priori uncertainty of their parameters and time boundaries require the development of new adaptive approaches for MRPs automatic detection (Samuel et al. 2021).

This study is aimed at the development of the new adaptive method for automated detection of MRPs as EEG markers of the well-known individual brain activity associated with voluntary movement preparation. The hypothesis of the study is that the search function reflects the presence of the initial and final time boundaries of the MRPs. First, an adaptive spectro-temporal decomposition of the EEG signals employing a number of band-pass filters (BPF) is performed. Only one of the adaptive BPFs is selected so that the filtered EEG signal has a frequency range corresponding to the maximum frequency spectrum of the target MRPs. The subsequent search of time boundaries of for low-amplitude target MRP pattern in time domain we carried out not in the original EEG signal, but in so preliminary filtered original EEG time series. Therefore, we ensured high sensitivity of the search algorithm. Based on the found time boundaries of the MRPs, time epochs corresponding to the voluntary motor preparation brain activity of a person are extracted from the original unfiltered multidimensional EEG. This allows to create an efficient machine learning dataset to classify the type of movement being prepared and designed to build the most reliable BCIs.

2 Method for automatic detection time boundaries of the MRPs

Registration of the multidimensional EEG

$$\mathbf{S}(t) = (S_1(t)\ \ S_2(t)\ \ \ldots\ \ S_J(t))^{\mathrm{T}} \tag{1}$$

was carried out at the same time intervals $t \in [t_0, t_k]$ on J standard leads (where t_0 and t_k are the initial and final time intervals; $^{\mathrm{T}}$ signifies transposition). The EEG $\boldsymbol{S}(T)$ (1) assumes the presence of a number of movement-related brain potentials that specifically reflect the voluntary motor preparation brain activity, where $T = t_k - t_0$ is the observed time for automated detection of MRPs. The time interval T was known a priori and corresponded to the duration of the target MRP pattern $T_p = t_{k,p} - t_{0,p}$, where $t_{0,p}$ and $t_{k,p}$ are the initial and final time boundaries of the MRP pattern. Thus, T and T_p were close in value, but $T_p < T$ is guaranteed.

Time boundaries of MRP patterns were detected in time domain. Criterion-based search reflected the presence of the time boundaries of the MRPs. Usually, the search sensitivity isn't sufficient for searching low-amplitude MRP patterns with a priori unknown parameters in noisy EEG signals. It is known that some parameters of MRP patterns and their spatial localizations are determined by the type of human mental activity (Amin et al. 2019). For instance, frequencies from 30 to 70 Hz (γ1 and γ2- frequencies) demonstrate high directional sensitivity to the type of motor activity being executed and correlate with the processes of selective attention. But it is the alpha frequencies (α-range) from 12 to 16 Hz of the frontal and central regions of the cerebral hemispheres that are closely related to the preparation for the execution of voluntary movements (Babiloni et al. 1999; Deiber et al. 2012; Kobler et al. 2020). It was shown that the maximum frequency power spectrum of narrow-band pattern of the named regions in the α range specifically reflect BCIs

compatible early conscious access to preparation of voluntary motor activity, related to the pre-motor potential (also known as Bereitschaftspotential or Readiness potential) (Shibasaki and Hallett 2006; Parés-Pujolràs et al. 2019; Braquet et al. 2020). So, it is advisable to run a preliminary search of the narrow-band MRP pattern in the individual frequencies related to the different type of movement-related brain activity of an individual at the observed moment. Preliminary filtering the original EEG in the frequency range maximum correspond to the frequency range of the target MRP pattern can provide a very high sensitivity for subsequent searching of time boundaries of this pattern.

Obviously, the modal frequencies of MRPs are a priori uncertain and can demonstrate a very high variability even during one experimental series. Therefore, the use of band-pass filter with a priori specified parameters would not provide maximum corresponding of the frequency range of the filtered EEG signal to the frequency range of the sought narrow-band MRP patterns at the observable time moment. For example, experimental studies confirmed the well-established fact (Zapała et al. 2020) that multiple executions of the same type of movement can significantly modify the frequency range of these patterns.

To transfer EEG signals from the temporal representation to the time–frequency representation, historically, a mathematical tool has been used based on the windowed Fourier transform and spatial filtering of oscillating components (Jusas and Samuvel 2019), or discrete or continuous wavelet transforms (Taran and Bajaj 2019), or multitaper spectral decomposition (Walden 2000; Babadi and Brown 2014), or empirical mode decomposition (EMD) (Huang et al. 1998; Bajaj and Pachori 2012). These methods allow to search for a specific brain pattern within the framework of various criteria functions (Shcherban et al. 2018, 2019; Bablani et al. 2019). Nowadays, wavelet decomposition and EMD are the most widely discussed frequency domain techniques in this case. But each method has some features that can be used to synthesize required adaptive BPF. It was considered that, depending on the type of cognitive load, physiological EEG rhythms can demonstrate multidirectional changes in narrow frequency bands. Thus, for example, preparation for the implementation of real movement is accompanied by changes both in low-frequency delta- (1–4 Hz) and alpha-ranges (8–12 Hz) of the EEG, and in higher-frequency beta- (13–35 Hz) and gamma (γ1, 35–45 Hz) frequencies (Onay and Köse 2019). For this reason, it is necessary that parameters of BPFs correspond to the spectrum characteristics of the most high-frequency rhythm of all frequency ranges related to the studied process of preparation for the execution of motor acts recorded at the interval T in target channels. It is still difficult to control parameters of the synthesized adaptive filter so that its bandwidth matches the narrow-band frequency range of the sought MRP pattern at the observable time moment.

It is known that such time series as EEG signal can be deconstructed in the time domain with the use of the Singular Spectrum Analysis (SSA) methodology into a sum of oscillatory components—reconstructed components (RC) (Golyandina and Zhigljavsky 2020). The frequency spectra of each RC depend on the number of SSA filters used in the decomposition and are ordered in ascending order. Thanks to this feature, SSA filters are adaptive to probabilistic changes in the original signal. This feature enabled us to solve, for example, the problems of extraction of multi-source brain activity using only single-channel recordings of electromagnetic brain signals (James and Lowe 2003), rejection of low-frequency artifacts in spontaneous EEG (Hu et al. 2017), high-quality suppression of high-frequency noise (Ghaderi et al. 2011) and high-precision filtering (Maddirala and Shaik 2016). To automatically remove low-frequency artifacts in the human EEG, an adaptive filter was synthesized as part of the development of portable telemedicine devices (Hu et al. 2017). In Ref. (Shcherban et al. 2020) the use of an adaptive band-pass SSA filter was considered mainly for increasing the sensitivity of the criterion function to search olfactory evoked patterns in the bioelectric activity of the rat's olfactory bulb. Another important aspect of the SSA, unlike many other methods, is that it works well even for small sample sizes (Hassani 2007; Hassani and Zhigljavsky 2009). For example, a short motor potential (40–80 ms) is formed in the primary motor cortex (M1) immediately before executing a voluntary movement, which is associated with the impulse of pyramidal cells to the motor end plates of the effector muscle, that is why this feature is important for automated detection of time boundaries of short MRPs.

The new method for detecting specific MRP patterns was as follows. At first it was considered that different type of human mental activity determines different spatial localization of EEG patterns (Amin et al. 2019). That is why only $J' < J$ EEG leads from the regions of interest were required for subsequent analyses. Applying SSA on the measurement interval T with a set of M filters the first of which is a low-pass filter (LPF), and the rest (M-1) are band-pass filters (BPF), each j-th ($j = \overline{1, J'}$)component $S_j(T)$ of multidimensional EEG $\mathbf{S}(T)$ required for subsequent analysis can be divided into M time series $S_j(T) = \left(\tilde{S}_{j,1}\ \ \tilde{S}_{j,2}\ \ \ldots\ \ \tilde{S}_{j,M}\right)^{\mathrm{T}}$ of the same dimension as the original data S_j (Golyandina and Zhigljavsky 2020). To reconstruct a system of simultaneous time series similar as the multidimensional EEG $\mathbf{S}(T)$ (1), the multidimensional SSA (MSSA) (Golyandina and Zhigljavsky 2020) can be used. But in each j lead the narrow-band MRP pattern has

different maximum frequency spectrum at the observed time moment (Xu et al. 2021). Therefore, the SSA decomposition of each j-th component $S_j(T)$ from (1) separately is more correct in comparison with the simultaneous MSSA decomposition of the original multidimensional EEG.

The frequency spectra $\Delta F_{j,1},\ldots,\Delta F_{j,M}$ of j,m-th ($j=\overline{1,J'}$; $m=\overline{1,M}$) reconstructed components (RC) $\tilde{S}_{j,1},\ldots,\tilde{S}_{j,M}$ depend on the number M of SSA filters used in the decomposition and are ordered in ascending order. The upper frequency limits of the spectra of the RCs satisfy $f_1^h \le f_2^h \le \cdots \le f_M^h$, where $f_M^h = 0.5f_s$ and f_s is the EEG sampling rate. In this case, the sum of all narrow-band RCs reconstructs the original series EEG $S_j(T)=\sum_{m=1}^{M}\tilde{S}_{j,m}(T)$, while the choice of only some of them allows us to perform frequency filtering of the original EEG signal. In Ref. (Shcherban et al. 2020), to simplify the synthesis procedure for the required adaptive band-pass filter, the narrow-band signal was restored by just one RC and the required BPF was synthesized. Considering that MRP pattern has the narrow-band frequency spectral characteristics we used the same approach further on. Varying of number M in the range $M\in[M_{\min};M_{\max}]$ leads to change in the bandwidth of each m-th filter. With an increase in M, the effective passbands of BPFs decrease. Also in Ref. (Golyandina and Zhigljavsky 2020), it is shown, that the amplitude-frequency characteristic (AFC) $A_m=\left|H_m\left(e^{j2\pi f'}\right)\right|=A_m(f',M)$ of a given M filter is a function of the M, where $H_m\left(e^{j2\pi f'}\right)=\sum_{n=0}^{MJ-1}h_{m,n}e^{-j2\pi f'n}$—the frequency response; h_m—the known impulse response of non-recursive SSA filter; $f'\in[0;\ 0.5]$—the given frequency. The choice of the given frequency step from the equality $f' = 1/f_s$ makes it possible to calculate the frequency response AFC $A_m(f,M)$ in the real frequency range $f\in[0;\ 0.5\,fs]$ with a discreteness of 1 Hz. So, thanks to known h_m in SSA decomposition it's easy to control the frequency spectra of each m-th RC $\tilde{S}_{j,m}(T)$. Varying the number M simultaneously changes each m-th ($m=\overline{1,M}$) SSA filter parameters in M-th decomposition ($M=\overline{M_{\min},M_{\max}}$) and so changes the frequency spectrum of the filtering j-th component $S_j(T)$ of the original EEG (1).

The AFC of SSA filters has a shape of a Gaussian function (GF) $g(f)=\exp\left(-\left(\hat{f}-f\right)^2\Big/2c^2\right)$. So, varying M leads to simultaneous changes in the modal frequency $\hat{f}$: $g_{\max}=g(\hat{f})=1$ of the Gaussian-like AFC and its bandwidth, determined by the c value (Golyandina and Zhigljavsky 2020). We also approximated the sought narrow-band MRP pattern in the frequency domain by the Gaussian shape. Therefore, it was required to select only one SSA band-pass filter (BPF) so that its Gaussian-like AFC maximally repeated the approximate MRP Gaussian function.

Parameters $\hat{f}$ and c alternatively can be interpreted by saying that the two inflection points f_L^{GF} and f_H^{GF} of the of the GF occur at $f_L^{GF}=\hat{f}-c$, $f_H^{GF}=\hat{f}-c$. Moreover, for the presented GF of unit height, it is true that $g\left(f_L^{GF}\right)=g\left(f_H^{GF}\right)=\exp(-1/2)$ for any pairs of numbers ($\hat{f}$, c). Consequently, a proximity measure of the pairs of inflection points of the GF of m-th BPF $\left(f_L^{BPF},f_H^{BPF}\right)$ and of the approximate MRP GF $\left(f_L^{RP},f_H^{RP}\right)$ fully reflect the proximity measure of the spectrum parameters of the m-th RC and the MRP pattern. Determination of the number m_{opt} from the criterion

$$m_{\text{opt}}(M)=\min_{\substack{m=\overline{1,M}\\ M=\overline{M_{\min},M_{\max}}}}\left\{\left(f_L^{BPF}-f_L^{RP}\right)^2+\left(f_H^{BPF}-f_H^{RP}\right)^2\right\}, \tag{2}$$

provides maximum correspondence of the spectrum parameters of the RC $\tilde{S}_{j,m_{\text{opt}}}(T)$ and of the sought narrow-band MRP pattern on the j-th lead ($j=\overline{1,J'}$) on the observed time interval T. In general, there are different numbers m_{opt} on the EEG leads. The preliminary filtering of the original EEG signals in the frequency range corresponding most to the frequency range of the MRP pattern provides the required sensitivity for subsequent searching of time boundaries of this pattern in time domain.

Subsequent search of time boundaries of the MRP pattern was carried out on the analysis of the multidimensional time series of RCs

$$\tilde{\mathbf{S}}(T)=\left(\tilde{S}_{1,m_{opt}}\ \ \tilde{S}_{2,m_{opt}}\ \ \ldots\ \ \tilde{S}_{J',m_{\text{opt}}}\right)^{\text{T}}, \tag{3}$$

where $\dim(\tilde{\mathbf{S}})=J'\times K$; $K=Tfs$—the time series length. By comparing two neighboring sliding time windows equal in volume and containing $J'\times n$ point sets ($n<<K$) the criterion-based search reflecting the degree of dynamic differences in $\tilde{\mathbf{S}}(T)$ (3) for each adjacent sliding pair of windows.

The criterion function was based on the calculation of the Hausdorff distance (HD) H. The HD is a measure of dissimilarity between two-point sets. It is commonly used in many domains like pattern matching, for example, in medical applications related to the evaluation of medical segmentations (Vizilter and Zheltov 2014; Taha and Hanbury 2015). The HD is the maximum of the non-symmetrically directed Hausdorff distances in both directions. In the considered approach, the directed Hausdorff distance H_d between two $J'\times n$ point sets $\tilde{\mathbf{S}}(T_i)$ and $\tilde{\mathbf{S}}(T_{i+1})$ from two i and $i+1$ neighboring time windows (where T_i, $T_{i+1}<<T$ and $T_i=T_{i+1}=n/fs$) is the maximum of the

Euclidean distances $\|\cdot\|$ from each point $\tilde{s}^{\langle i\rangle} \in \tilde{\mathbf{S}}(T_i)$ to its nearest neighbor $\tilde{s}^{\langle i+1\rangle} \in \tilde{\mathbf{S}}(T_{i+1})$:

$$H_d\left[\tilde{\mathbf{S}}(T_i), \tilde{\mathbf{S}}(T_{i+1})\right] = \max_{\tilde{s}^{\langle i\rangle} \in \tilde{\mathbf{S}}(T_i)} \left\{ \min_{\tilde{s}^{\langle i+1\rangle} \in \tilde{\mathbf{S}}(T_{i+1})} \left\{ \left\| \tilde{s}^{\langle i\rangle}, \tilde{s}^{\langle i+1\rangle} \right\| \right\} \right\}.$$

So, HD H is given by

$$H\left[\tilde{\mathbf{S}}(T_i), \tilde{\mathbf{S}}(T_{i+1})\right] = \max\left\{H_d\left[\tilde{\mathbf{S}}(T_i), \tilde{\mathbf{S}}(T_{i+1})\right], H_d\left[\tilde{\mathbf{S}}(T_{i+1}), \tilde{\mathbf{S}}(T_i)\right]\right\}. \quad (4)$$

The HD (4) is calculated for all adjacent windows. Then, if there is an initial or final boundary of the desired MRP pattern in any pair of the neighboring sliding windows, the measure of the dissimilarity of these two-point sets increase, the criterion function H (4) acquires its local maximum value. The size n of the sliding time window is selected so that the a priori known duration of the MRP pattern is guaranteed to exceed the value of n/f_s. We synthesized the following algorithm for automatic detection of time boundaries of the target RP patterns (Fig. 1).

Taking into consideration the spatial localization of the studied human brain activity type, $J' < J$ EEG signals are selected from the original multidimensional EEG. Based on the Fast Fourier transform of each j-th ($j = \overline{1, J'}$) original signal $S_j(T)$ on the observed time T power spectral density (PSD) functions are calculated. Then, in the frequencies of interest $f \in [f_L, f_H]$ the modal frequencies f_j^{RP}: $P_j(f_j^{RP}) = 1$ of the MRPs are detected, where $P_j(f)$ denotes normalized PSD. It is easy to calculate inflection point pairs $\left(f_L^{RP}, f_H^{RP}\right)_j$ of the approximate GFs of the $P_j(f)$ of MRPs. Also, by varying the number M in the range $M \in [M_{\min}; M_{\max}]$ the one optimal BPF with number $(m_{\text{opt}}(\text{M}))_j$ from the criterion (2) is selected. In this case the spectrum of the filtering j, m-th RC $\tilde{S}_{j,m_{\text{opt}}}(T)$ most closely matches the spectrum of the target MRP pattern, observed at the j-th EEG lead. The multidimensional so preliminary filtering signal $\tilde{\mathbf{S}}(T)$ (3) is divide into K/n of time windows of the same dimensions $J' \times n$. The HD (4) is calculated for all adjacent windows.

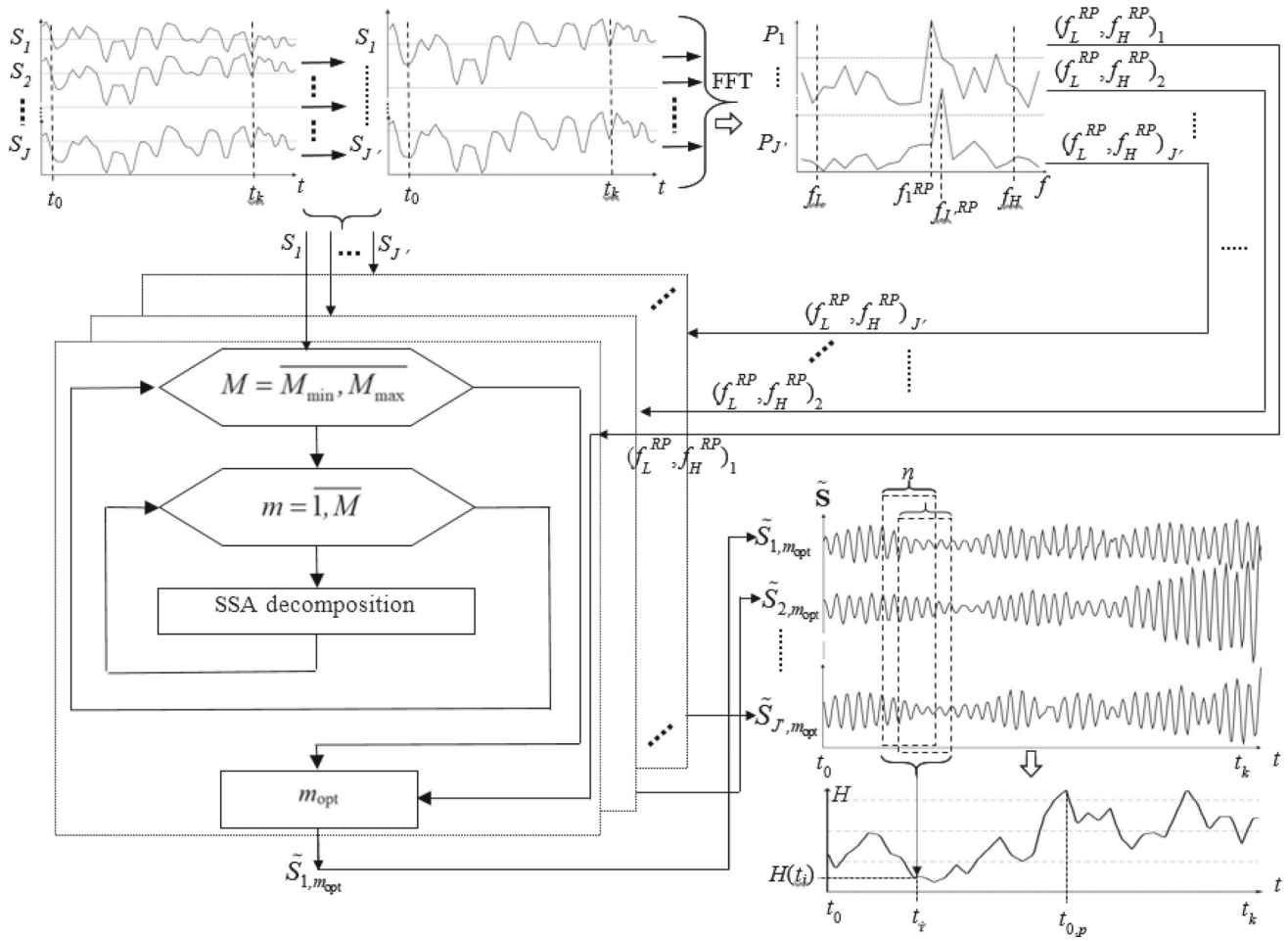

Fig. 1 Developed algorithm for automatic detection time of boundaries of the MRP

Then, if there is an initial or final boundary of the desired pattern in any of the neighboring windows, the criterion function H (4) acquires its local maximum value.

Based on the found time boundaries of the MRPs epochs corresponding to the voluntary movement-related brain potentials, in particular, the Readiness potentials are extracted from the original unfiltered multidimensional EEG (1). We apply the above proposed method to movement and motor imagery dataset that we have previously obtained and analyzed using other methods to create new asynchronous and stimulus-independent Brain-computer interfaces (Shepelev et al. 2018; Lazurenko et al. 2019).

3 Research methodology

To test the developed tools, the following experimental studies were performed. The surveys involved 16 healthy volunteers (11 men and 5 women) with the average age of 21. In accordance with ethical standards of the 1964 Helsinki Declaration and its later amendments and the ethics committee of Southern Federal University, they all signed a voluntary consent protocol for participation in the research.

Further experimental studies were carried out only on voluntary motor activity related to the pre-movement Readiness potential (RP) (or Bereitschaftspotential). The fact of preparation for movement execution by a person is obvious and it is easy to test with the developed tools on the RP patterns compared with the motor imagery patterns. For selected type of motor activity, the alpha-range (mu-rhythm) frequencies from $f_L = 12$ to $f_H = 16$ Hz of the central regions of the cerebral hemispheres are closely related to the preparation for the execution of voluntary movements. It is obvious that the initial moment *ta* of the actual hand movement initialization practically coincides with the terminal moment of the target pre-motor RP pattern associated with the preparation for the motor act and $t_a = t_{k,p} = t_k$. For this reason, in each study sample, we were searching for only the initial boundaries of the pre-motor RP patterns of a person $t_{0,p}$. It is generally accepted that RP patterns associated with the direct preparation of a specific plan for executing voluntary movements, as a rule, do not exceed 500 ms (Kobler et al. 2020). In this regard, the detection of the desired RP patterns was carried out at $T = 1000$ ms preceding the moment of actual initialization of the hand movement t_a and $T_p < T$ is guaranteed.

During the electrophysiological tests, the participants were in a comfortable position (in a chair) in a specially equipped light and sound-proof Faraday chamber. The subjects executed real movements with their legs, right and left arms at a voluntary pace with the eye fixed on the placemark in the center of the screen. The movements of the upper limbs alternated with a state of rest when the subject was motionless for some random time with their eyes open. In this case, the EEG was recorded continuously—both at rest and in preparation for the execution of the actual movement. Movement execution with each arm was covered around 25 cycles for each subject. Figure 2 shows a fragment of the timing diagram of an experimental session for one type of movement.

The EEG $\mathbf{S}(t)$ (1) was recorded relative to the ear reference electrodes (combined reference) with an Encephalan-131–03 amplifier (Medikom MTD, Taganrog) from $J = 17$ standard channels (F7, F8, F3, Fz, F4, C3, Cz, C4, P3, Pz, P4, O1, O2, T3, T4, T5, T6) in accordance with the international system "10–20". The EEG sampling rate was $f_s = 250$ Hz for each of the recording channels. The first and second harmonics of the 50 and 100 Hz power supply were removed using a notch filter.

In parallel, an electromyogram (EMG) was recorded on the superficial muscles flexing the forearm in the elbow joint (*m. Brachioradialis*) and the superficial flexors of the fingers (*m. Flexor digitorum superficialis*). The bipolar electromyogram was used to form event markers synchronized with the EEG channels. Each EMG channel was filtered in the frequency band of 1–4 Hz. As a result, a smoothed myographic spindle was formed. The events of the actual initiation of movement execution were set automatically when the threshold amplitude of 10 μV was reached on the ascending front of the smoothed EMG spindle. Thus, the initial moment t_a of the actual movement of arms was recorded quite accurately by means of bipolar EMG channels. To detect and subsequently reject artifacts associated with eye movement and blinking automatically, an electro-oculogram (horizontal and vertical EOG) was recorded. The dataset is available at (http://neuro.sfedu.ru/eeg_premotor_pattern_sfedu_2020/).

4 Computational results

4.1 Time boundaries detecting results

The correctness of the decisions made were verified with standard statistical tests and machine learning algorithms. The developed method was used to detect the initial time boundaries of the pre-motor RP patterns of 16 persons in each trial of movement execution both with the right and left arm.

For the right arm, the target leads of the left hemisphere F3, C3, P3 and T3 responsible for the development of the pre-motor pattern were selected, and for the left arm—the EEG leads F4, C4, P4 and T4 ($J' = 4$ in both cases). The maximum permissible number of filters is determined by $M_{\max} \leq 0.5\,K$, where the length of the time series was $K = 250$. Considering the frequency range of RPs [12;16]

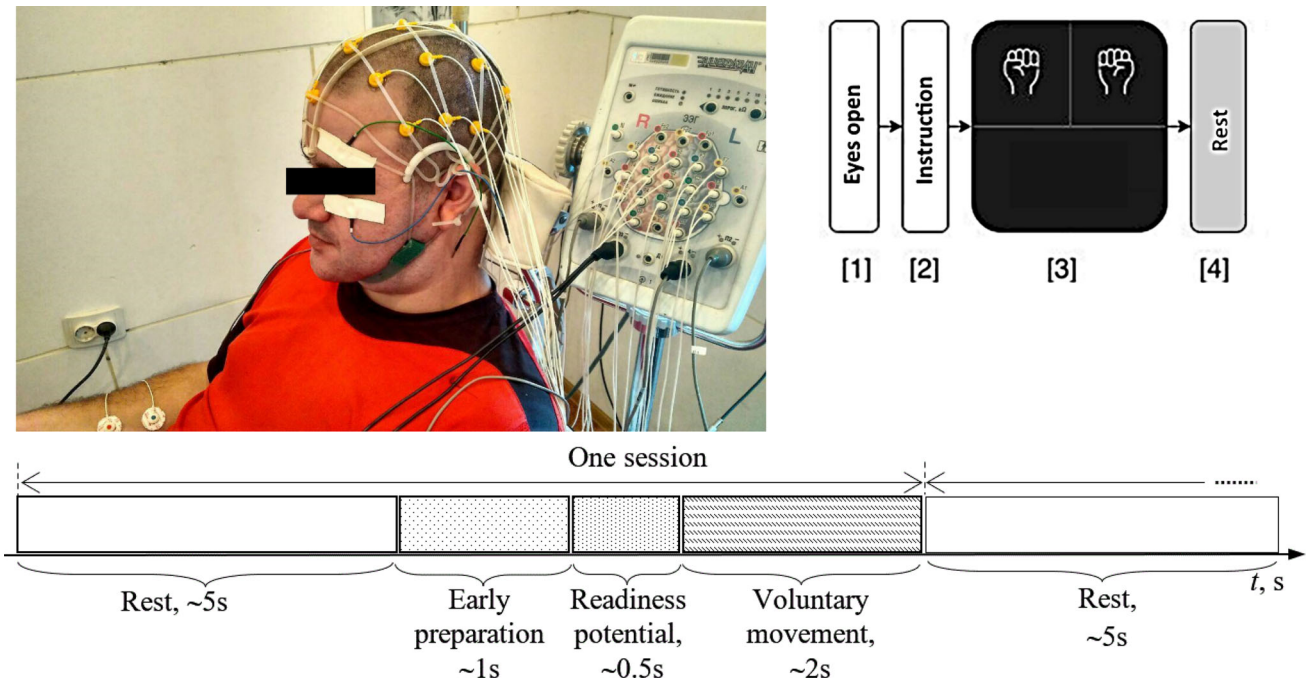

Fig. 2 Timing representation of a scenario with the participation of volunteers in the task of movement execution. [1] Rest with eyes open; [2] Instructions; [3] Movement execution with left or right arm; [4] Rest after movement execution. A time diagram of an experimental session for voluntary movement execution

Hz in the SSA decomposition of selected single-channel EEG components $S_j(T)$ we used $M_{\max} = 70$, $M_{\min} = 4$. Spectrum parameters of synthesized adaptive SSA BPFs and of sought narrow-band RP patterns matched well. Three typical examples of the preliminary filtering of j-th component $S_j(T)$ from one target EEG channel shown on Fig. 3.

To verify the adaptation properties of the selected SSA BPFs, we also used six-order Butterworth BPF with the constant passband [12;16] Hz for comparison. The spectral composition of the RPs recorded for the actual movement execution preparation in the shown examples is significantly different. In the graphs (Fig. 3b) the modal frequency f_j^{RP}: $P_j(f_j^{RP}) = 1$ of the RP pattern shifted to the lowest frequency of alpha-rhythm (normalized in range $[f_L; f_H]$ PSD $P_j(f)$ shown with bold solid lines). In the other two examples, the modal frequency of RP patterns is in the middle of the frequency range of interest (Fig. 3a) or close to the upper frequency limits (Fig. 3c). The top graphs in Fig. 3 also show normalized amplitude-frequency characteristic (AFC) A_m of the selected $m = m_{\text{opt}}$ BPFs, normalized AFC A_B of the Butterworth BPF and approximate GFs (AGF) of the PSD $P_j(f)$ of RP patterns. The dotted lines in the graphs at the bottom of Fig. 3 demonstrate normalized PSD $P_j^{RC}(f)$ of the RCs $\tilde{S}_{j,m_{\text{opt}}}(T)$ (solid lines) and normalized PSD $P_j^{B}(f)$ of the filtering with Butterworth BPF j-th single-channel EEG time series (dotted lines). It is clear that the spectrum of RCs $\tilde{S}_{j,m_{\text{opt}}}(T)$ closely matches the spectrum of the target RP patterns and, therefore, the developed algorithm made it possible to obtain individual optimal SSA BPF for the given examples of RPs. Butterworth BPF with a priori specified parameters did not provide maximum correspondence to of the frequency range of the filtered EEG signal to the frequency range of the RP patterns at the observed time moment.

When searching for the initial boundary of the RP patterns $t_{0,p}$ the width of the sliding window was 100 ms, and the overlap coefficient of the adjacent windows was 0.9. (Fig. 4a–c) shows 3 typical examples of the HD (4) graphs carried out at observed time interval $T = t_0 = 1000$ ms preceding the moment $t_a = t_{k,p} = t_k = 0$ of actual initialization of the right arm movement from one experimental session of a person.

We detected that the first maximum value of the HD corresponds to the initial boundary of the target RP pattern $t_{0,p}$ while preparing for the actual movement execution. In Ref. (Kobler et al. 2020) generally accepted that RP patterns, as a rule, do not exceed 500 ms. A detailed analysis demonstrated that there are significant fluctuations in $t_{0,p}$ coupled with the temporal characteristics of the RPs. In some cases, the $t_{0,p}$ exceeded 500 ms and were, on average, 374 ± 130 ms for the right arm and 348 ± 100 ms for the left arm. (Fig. 5) shows box plot of RPs initial time boundaries $t_{0,p}$ in sec for both arms.

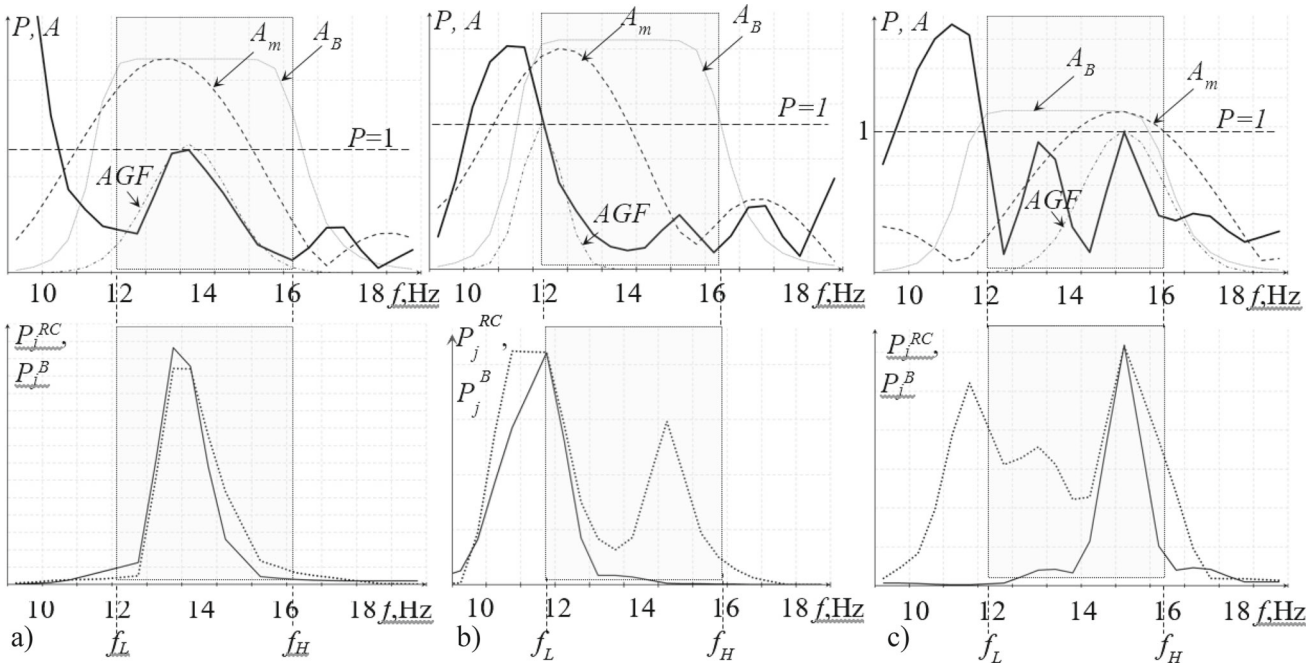

Fig. 3 The top graphs show PSD function $P_j(f)$ (bold solid lines), normalized AFC A_m, $m = m_{opt}$ of the selected BPFs, normalized AFC A_B of the Butterworth BPF and approximate GFs of the PSD $P_j(f)$ of RP patterns. The bottom graphs show normalized PSD $P_j^{RC}(f)$ of the RCs $\tilde{S}_{j,m_{opt}}(T)$ (solid lines) and normalized PSD $P_j^B(f)$ of the filtering with Butterworth BPF EEG component S_j (dotted lines)

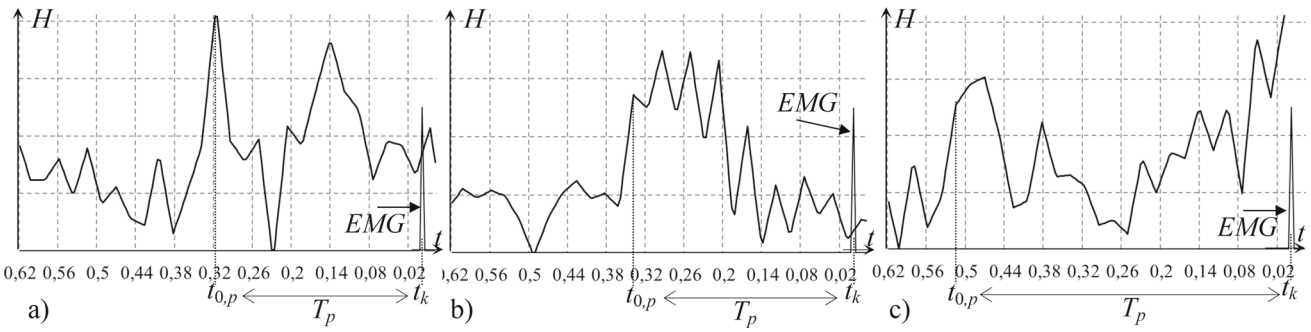

Fig. 4 Three examples of the HD function (4) from one experimental session of a person

The well-known fact was also confirmed (Hu et al. 2017; Pereira et al. 2019), according to which the frequency ranges associated with the preparation for movement can demonstrate a certain variability in the assessment of single trials even within the same subject. It is for this reason that the use of frequency filters with a priori given parameters seems to be ineffective.

4.2 Results of discrete classification problems

Based on the found time boundaries of the MRPs, time epochs corresponding to the voluntary motor preparation brain activity of a person were extracted from the original unfiltered multidimensional EEG signals. The hypothesis of the study was that this fact allows to create an efficient machine learning dataset to classify the type of movement being prepared by a person. We validated this hypothesis with standard machine learning algorithms. We checked the quality of the separation of time epochs related to the state of rest of each person and epochs pertaining to the preparation for the execution, therefore, containing RP patterns. Based on the detected time boundaries of the RP patterns for each trial of movement execution by each person correct time epochs $[t_{0,p}; t_k]$ were extracted from the original EEG. Thus, we prepared data sets of classes namely the "Modified method (MM), right arm (RA)" and the "MM, left arm (LA)." Also, we had the analogous data sets of classes namely the "Standard method (SM), RA" and "SM, LA," where detection of initial time boundaries was carried out as constant $t_{0,p}^{\text{Standard}} = 500$ ms (Kobler

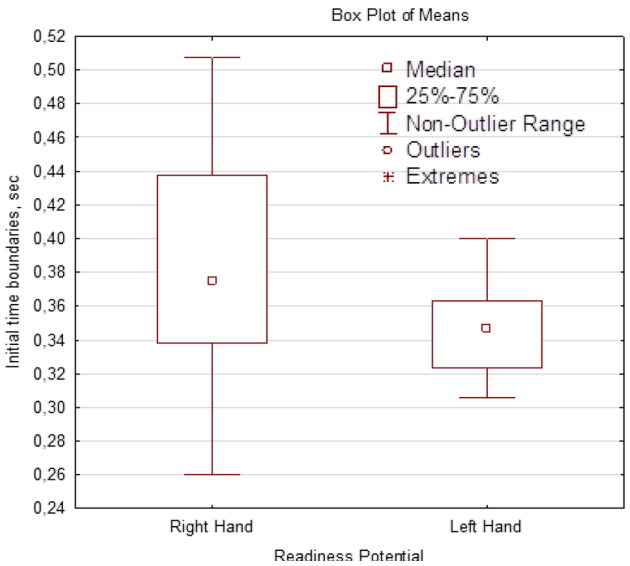

Fig. 5 Box plot of Mean parameters of the initial time boundaries of two target movement-related EEG patterns

et al. 2020). Final time boundaries of time epochs t_k were the same as in the samples of "Modified method." For each person, we also prepared data sets of class "Rest," each containing 25 samples of 500-ms epochs selected randomly in each cycle of the experimental series in intervals corresponding to the state of operative rest before and after a single limb movement (see Fig. 2). Therefore, it was possible to solve the problem of discrete classification with standard machine learning algorithms.

At the first stage of calculations, best machine learning (ML) models and their best parameters were selected. Standard ML models Random Forest, Support Vector Machine, k-nearest neighbors, Gradient boosting decision trees (GBDT), Multilayer Perceptron and Classifier, based on linear discriminant analysis from the Python. Scikit-learn library were used. In total, about 300 reference features of different types from selected EEG epochs were calculated and synthesized—temporal, frequency, and frequency-temporal, as well as spatial. Additionally, the standardization of each selected feature in the data set was performed by removing the mean and scaling it to a unit variance. Detection of the best parameters for each ML model was provided using scikit-learn's GridSeacrh method. The selected classification models had sufficient generalizing ability which excluded the possibility of their undertraining or retraining. It turned out that the classification model of GBDT with parameters {deviance loss function, the minimum number of samples required to split an internal node and required to be in a leaf node equals 3, number of estimators equals 50} was the most efficient among the trained methods. The most important features were slopes of the regression lines, intersections of regression lines, correlation coefficients, standard errors of the estimated slopes, standard errors of the calculated intersection points assuming residual normality between the non-filtering single-channel EEG time series.

At the second stage, the binary discrete classification problem on standard datasets of two target states {"SM, RH/LH"—"Rest"} was solved. As expected, the maximum accuracy of binary classification in Stratified ShuffleSplit cross-validation at this stage was low and averaged at only 62% for the right arm and 67% for left arm. (Fig. 6a) shows box plot of accuracy of the solved classification problem. There were also significant variations in the classification accuracy—from 48 to 82% among different subjects. Interindividual differences are known to make a significant contribution to the assessment of subsets of EEG channels that usually differ significantly. In fact, the low average classification accuracy in the general set of data observed at the first calculation stage is most likely explained by the fact that, in addition to the target RP patterns, the composition of the epochs T = 500 ms of the "SM, RH/LH" classes includes other electrographic patterns not related to the current motor task.

Then was solved the binary discrete classification problem of the same two target states but on modified data sets {"MM, RH/LH"—"Rest"}. The GBDT model with the best parameters was retrained, and its accuracy was verified during cross-validation. The accuracy of the binary classification for Modified method increased in comparison with Standard method on average by 32% for the right and 26% for left arm (see Fig. 6b). At the same time, the maximum observed classification accuracy on modified datasets calculated separately for each person, in some cases, increased to 99% for the right arm and to 100% for the left arm.

Then data sets of classes "MM, RH" and "MM, LH" had been merged in one class "MM, Movement execution." Classes "SM, RH" and "SM, LH" were also combined in one class "SM, Movement execution." Two binary discrete classification problems of classes {"MM, Movement execution"—"Rest"} and classes {"SM, Movement execution"—"Rest"} were solved. The accuracy of the binary classification categorized by "Method" was significantly higher for Modified method and amounted to average 94% ± 6% (see Fig. 6, c).

(Fig. 7a) shows quantile–quantile plot of the accuracy categorized by Method with Gamma distribution reflecting two probability movement-related EEG pattern distributions by comparing their quantiles against each other. MM had accuracy $89 + 3.9 \times x$ and SM had accuracy only $55 + 8.9 \times x$ (Shape par. $x = 1,\ 2$). (Fig. 7b) shows quantile–quantile plot of accuracy, categorized by Method and State (Rest and Movement preparation) with Gamma

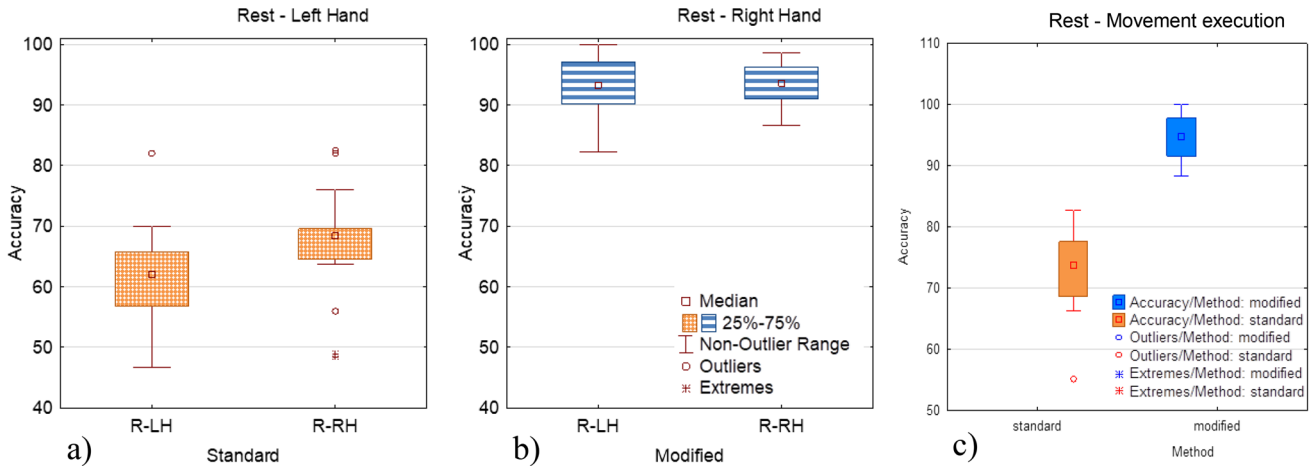

Fig. 6 Box plot of accuracy of the binary discrete classification of two target movement-related EEG patterns: **a** classes "SM, RA/LA" and "Rest (R)"; **b** classes "MM, RA/LA" and "Rest (R)"; **c** classes "SM/MM, Movement execution" and "Rest"

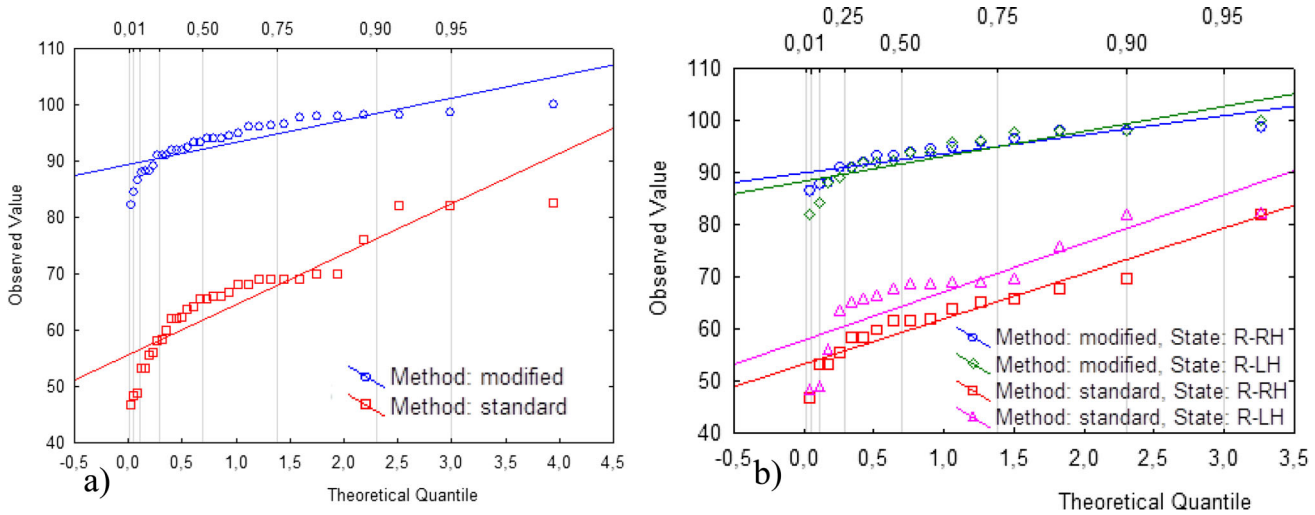

Fig. 7 Box plot of quantile–quantile plot of accuracy: **a** Categorized by "Method" with Gamma distribution (Gamma shape = 1,2); **b** Categorized by "Method" and State (Rest and Movement preparation) with Gamma distribution

distribution. MM had accuracy 89/88 for RH/LH and SM had accuracy only 53/57 for RH/LH.

5 Discussion

Results highlighted the main features of the work and proved the hypothesis of the study that detailed determination of time boundaries of MRP patterns reflected in EEG signals allows increasing the classification accuracy of the state of rest of a person and of the state associated with movement preparation. Therefore, developed method is capable of automatic detection of MRPs as a marker of voluntary motor EEG activity of an individual. Application of a synthesized method obtain to correctly extract from EEG signals of those time epochs that containing the desired pre-motor MRPs. Thanks to this fact, it is possible to prepare an efficient machine learning dataset and, therefore, to increase the accuracy of the subsequent classification of the type of movement executed by a person at the observable time moment.

The required search sensitivity of time boundaries of MRPs is achieved through preliminary filtering of the original EEG signals. SSA methodology allows to take into account significant fluctuations in spatial-frequency characteristics of the EEG in terms of voluntary movements execution (Mammone et al. 2020; Wang et al. 2020; Santos et al. 2020) and, therefore to control parameters of the synthesized adaptive filter so that to obtain individual optimal SSA band-pass filter with bandwidth closely matching the spectrum of the desired MRP at the observed moment. We showed that Butterworth BPF with a priori

specified parameters did not provide maximum correspondence of the frequency range of the filtered EEG signal to the frequency range of the sought narrow-band RP pattern at the observed time moment.

We made a statistical analysis of the results and showed that duration of RP patterns was, on average, 374 ± 130 ms for the right hand and 348 ± 100 ms for the left hand. We have emphasized the well-known fact (Hu et al. 2017; Pereira et al. 2019) that frequency ranges associated with the preparation for movement can demonstrate a certain variability in the assessment of single trials even within the same subject. It is for this reason that the use of frequency filters with a priori given parameters seems to be ineffective. Our results also indicate that the information processes of the brain related to pre-movement EEG patterns in particular can be seen as a promising direction for improving Brain-Computer Interfaces (Bocquelet et al. 2016; Cooney et al. 2018). The results obtained in this study are consistent with the findings related to the fact that subjective desire to perform a movement (W-judgment) occurs 300–500 ms before it is execution (Libet et al. 1983, Alexander et al. 2014; Drozdzewska et al. 2017; Kobler et al. 2020).

We also used standard machine learning algorithms. We checked the quality of the separation of time epochs from original EEG signals related to the state of rest of each person and epochs pertaining to the preparation for the execution, i.e., containing RP patterns. A detailed determination of initial time boundaries of the pre-movement RP patterns allowed to extract from original EEG epochs, containing only the desired pre-motor brain patterns. The main goal of analysis was to prove, that classification accuracy on the data sets with determined time boundaries of epochs, higher than classification accuracy on the data sets with standard time intervals (500 ms) of epochs containing RP patterns. On average, the developed method has increased the accuracy of the binary classification by 32% for the right and 26% for the left arm. The maximum observed classification accuracy calculated separately for each subject, in some cases, increased to 99% for the right arm and to 100% for the left arm. Results obtained allow us to prove that the method of adaptive search we developed is able to effectively and reliably determine the time intervals when the functional state of brain structures transit from idle activity or default mode to the actual motor task. These transitions between states are important for identifying the presence of a target movement preparation and motor imagery EEG patterns potentially suitable for control in the circuit of "Brain-computer" or "Brain-to-Brain" systems.

6 Conclusion

This study presents a new method for automatic detection in the spontaneous bioelectric activity of the human brain of specific, invariant patterns of activity associated with the execution of voluntary motor acts by individuals. An adaptive band-pass filter with bandwidth closely matching the spectrum of the desired pre-motor EEG patterns preceding the execution of actual movements was synthesized based on Singular Spectrum Analysis methodology. The preliminary filtering of the original EEG signals provides the required sensitivity for subsequent searching of time boundaries of this pattern in time domain. The search function calculates the Hausdorff distance between two neighboring sliding time windows and reflects the presence of time boundaries of the pattern. If there is an initial or final boundary of the desired pattern in any pair of the neighboring sliding windows, the criterion function acquires its local maximum value.

The correctness of the developed method was confirmed with standard machine learning tools through the validation of the adaptive search method carried out on the general set of initial data. Computational experiments have convincingly demonstrated that the use of the developed method is possible to provide reliable detection of induced pre-motor EEG patterns and the correct determination of their time intervals. Extracting from original EEG signals of those epochs, that containing only the desired pre-motor brain patterns made it possible to increase the accuracy of binary classification for all subjects without exception by 29% on average and reach maximum values of 99% for the right arm and to 100% for the left arm with some subjects.

The developed method can be a reliable tool for solving applied problems of neural control in the BCIs circuit, as well as increasing the overall reliability of Neural interfaces for various purposes. We consider potential brain signals such as movement-related EEG patterns as well as the goals of BCI-based therapeutic applications. These useful BCI applications rely mostly on original and adaptive signal-processing technologies.

Acknowledgments For Southern Federal University Strategic Academic Leadership Program ("Priority 2030").

Funding This work was supported by the Russian Science Foundation (RSF) in the framework of "Development of stimulus-unrelated brain-computer interface for disabled people rehabilitation" project (No. 20-19-00627, 2020 -2022).

Data availability http://neuro.sfedu.ru/eeg_premotor_pattern_sfedu_2020/.

Declarations

Conflict of interest No conflict of interest.

Human and animals' participants In accordance with ethical standards of the 1964 Helsinki Declaration and its later amendments, all volunteers signed a voluntary consent protocol.

References

Abiri R, Borhani S, Sellers EW, Jiang Y, Zhao X (2019) A comprehensive review of EEG-based brain–computer interface paradigms. J Neural Eng. https://doi.org/10.1088/1741-2552/aaf12e

Alexander P, Schlegel A, Sinnott-Armstrong W, Roskies A, Tse PU, Wheatley T (2014) Dissecting the readiness potential. Surround Free Will Philos Psychol Neurosci. https://doi.org/10.1093/acprof:oso/9780199333950.003.0011

Amin SU, Alsulaiman M, Muhammad G, Mekhtiche MA, Hossain MS (2019) Deep Learning for EEG motor imagery classification based on multi-layer CNNs feature fusion. Futur Gener Comput Syst 101:542–554. https://doi.org/10.1016/j.future.2019.06.027

Babadi B, Brown EN (2014) A review of multitaper spectral analysis. IEEE Trans Biomed Eng 61(5):1555–1564. https://doi.org/10.1109/TBME.2014.2311996

Babiloni C, Carducci F, Cincotti F, Rossini PM, Neuper C, Pfurtscheller G, Babiloni F (1999) Human movement-related potentials vs desynchronization of EEG alpha rhythm: a high-resolution EEG study. Neuroimage 10(6):658–665. https://doi.org/10.1006/nimg.1999.0504

Bablani A, Edla DR, Tripathi D, Cheruku R (2019) Survey on brain-computer interface: an emerging computational intelligence paradigm. ACM Comput Surv (CSUR) 52(1):1–32. https://doi.org/10.1145/3297713

Bajaj V, Pachori RB (2012) EEG signal classification using empirical mode decomposition and support vector machine. Adv Intell Soft Comput. https://doi.org/10.1007/978-81-322-0491-6_57

Bocquelet F, Hueber T, Girin L, Chabardès S, Yvert B (2016) Key considerations in designing a speech brain-computer interface. J Physiol Paris 110(4):392–401. https://doi.org/10.1016/j.jphysparis.2017.07.002

Braquet A, Bayot M, Tard C, Defebvre L, Derambure P, Dujardin K, Delval A (2020) A new paradigm to study the influence of attentional load on cortical activity for motor preparation of step initiation. Exp Brain Res 238(3):643–656. https://doi.org/10.1007/s00221-020-05739-5

Chen C, Zhang J, Belkacem AN, Zhang S, Xu R, Hao B et al (2019) G-causality brain connectivity differences of finger movements between motor execution and motor imagery. J Healthc Eng. https://doi.org/10.1155/2019/5068283

Colamarino E, Pichiorri F, Mattia D, Cincotti F (2018) Bipolar filters improve usability of brain-computer interface technology in post-stroke motor rehabilitation. In: Proceedings of the 4th international conference on neurorehabilitation (ICNR2018), Pisa, Italy, pp 911–914. https://doi.org/10.1007/978-3-030-01845-0_183

Cooney C, Folli R, Coyle D (2018) Neurolinguistics research advancing development of a directspeech brain-computer interface. iScience 8:103–125. https://doi.org/10.1016/j.isci.2018.09.016

Craik A, He Y, Contreras-Vidal JL (2019) Deep learning for electroencephalogram (EEG) classification tasks: a review. J Neural Eng 16(3):031001. https://doi.org/10.1088/1741-2552/ab0ab5

Deiber MP, Sallard E, Ludwig C, Ghezzi C, Barral J, Ibañez V (2012) EEG alpha activity reflects motor preparation rather than the mode of action selection. Front Integr Neurosci 6:59. https://doi.org/10.3389/fnint.2012.00059

Drozdzewska A (2017) Free will—between philosophy and neuroscience. In: The human sciences after the decade of the brain, Academic Press, pp 42–60. https://doi.org/10.1016/B978-0-12-804205-2.00004-5

Eidel M, Kübler A (2020) Wheelchair control in a virtual environment by healthy participants using a P300-BCI based on tactile stimulation: training effects and usability. Front Hum Neurosci 14:265. https://doi.org/10.3389/fnhum.2020.00265

Freer D, Yang GZ (2020) Data augmentation for self-paced motor imagery classification with C-LSTM. J Neural Eng 17(1):016041. https://doi.org/10.1088/1741-2552/ab57c0

Golyandina N, Zhigljavsky A (2020) Singular Spectrum Analysis for Time Series (SpringerBriefs in Statistics). Springer Nature, Berlin. https://doi.org/10.1007/978-3-662-62436-4

Ghaderi F, Mohseni HR, Sanei S (2011) Localizing heart sounds in respiratory signals using singular spectrum analysis. IEEE Trans Biomed Eng 58:3360–3367. https://doi.org/10.1109/TBME.2011.2162728

Hassani H (2007) Singular spectrum analysis: methodology and comparison. J Data Sci 5(2):239–257. https://doi.org/10.6339/JDS.2007.05(2).396

Hassani H, Zhigljavsky A (2009) Singular spectrum analysis: methodology and application to economics data. J Syst Sci Complex 22(3):372–394. https://doi.org/10.1007/s11424-009-9171-9

Huang NE et al (1998) The empirical mode decomposition and the Hilbert spectrum for non-linear and non stationary time series analysis. Proc Royal Soc Lond A 454:903–995. https://doi.org/10.1098/rspa.1998.0193

Hu H, Guo S, Liu R, Wang P (2017) An adaptive singular spectrum analysis method for extracting brain rhythms of electroencephalography. PeerJ 5:e3474. https://doi.org/10.7717/peerj.3474

James CJ, Lowe D (2003) Extracting multisource brain activity from a single electromagnetic channel. Artif Intell Med 28:89–104. https://doi.org/10.1016/s0933-3657(03)00037-x

Jin J, Allison BZ, Kaufmann T, Kübler A, Zhang Y, Wang X, Cichocki A (2012) The changing face of P300 BCIs: a comparison of stimulus changes in a P300 BCI involving faces, emotion, and movement. PLoS ONE 7(11):e49688. https://doi.org/10.1371/journal.pone.0049688

Jusas V, Samuvel SG (2019) Classification of motor imagery using combination of feature extraction and reduction methods for brain-computer interface. Inf Technol Control 48(2):225–234. https://doi.org/10.5755/j01.itc.48.2.23091

Kobler RJ, Kolesnichenko E, Sburlea AI, Müller-Putz GR (2020) Distinct cortical networks for hand movement initiation and directional processing: an EEG study. Neuroimage 220:117076. https://doi.org/10.1016/j.neuroimage.2020.117076

Kübler A, Rupp R, Kleih S (2021) P300 BCI for persons with spinal cord injury: A BCI in search of an application?. In: Neuroprosthetics and Brain-Computer Interfaces in Spinal Cord Injury: A Guide for Clinicians and End Users. Springer, Cham, pp 193–216. https://doi.org/10.1007/978-3-030-68545-4_8

Lazurenko DM, Kiroy VN, Aslanyan EV, Shepelev IE, Bakhtin OM, Minyaeva NR (2018) Electrographic properties of movement-related potentials. Neurosci Behav Physiol 48(9):1078–1087. https://doi.org/10.1007/s11055-018-0670-9

Lazurenko DM, Kiroy VN, Shepelev IE, Podladchikova LN (2019) Motor imagery-based brain-computer interface: neural network approach. Opt Memory Neural Netw 28(2):109–117. https://doi.org/10.3103/S1060992X19020097

Lee WH, Kim E, Seo HG, Oh BM, Nam HS, Kim YJ, Bang MS (2019) Target-oriented motor imagery for grasping action: different characteristics of brain activation between kinesthetic

and visual imagery. Sci Rep 9(1):1–14. https://doi.org/10.1038/s41598-019-49254-2
Li C, Jia T, Xu Q, Ji L, Pan Y (2019) Brain-computer interface channel-selection strategy based on analysis of event-related desynchronization topography in stroke patients. J Healthc Eng. https://doi.org/10.1155/2019/3817124
Libet B, Gleason CA, Wright EW, Pearl DK (1983) Time of conscious intention to act in relation to onset of cerebral activity (readiness-potential): the unconscious initiation of a freely voluntary act. Brain 106(3):623–642. https://doi.org/10.1007/978-1-4612-0355-1_15
Maddirala AK, Shaik RA (2016) Motion artifact removal from single channel electroencephalogram signals using singular spectrum analysis. Biomed Signal Process Control 30:79–85. https://doi.org/10.1016/j.bspc.2016.06.017
Mammone N, Ieracitano C, Morabito FC (2020) A deep CNN approach to decode motor preparation of upper limbs from time–frequency maps of EEG signals at source level. Neural Netw 124:357–372. https://doi.org/10.1016/j.neunet.2020.01.027
McFarland DJ, Daly J, Boulay C, Parvaz MA (2017) Therapeutic applications of BCI technologies. Brain-Comput Interfaces 4(1–2):37–52. https://doi.org/10.1080/2326263X.2017.1307625
Onay FK, Köse C (2019) Power spectral density analysis in alfa, beta and gamma frequency bands for classification of motor EEG signals. In: 2019 27th signal processing and communications applications conference (SIU), pp 1–4. https://doi.org/10.1109/SIU.2019.8806385
Parés-Pujolràs E, Kim YW, Im CH, Haggard P (2019) Latent awareness: early conscious access to motor preparation processes is linked to the readiness potential. Neuroimage 202:116140. https://doi.org/10.1016/j.neuroimage.2019.116140
Pereira J, Direito B, Sayal A, Ferreira C, Castelo-Branco M (2019) Optimization of a motor imagery paradigm for self-modulation of bilateral premotor interhemispheric functional connectivity in fMRI neurofeedback. In: Mediterranean conference on medical and biological engineering and computing, pp 1743–1751. https://doi.org/10.1007/978-3-030-31635-8_212
Samuel OW, Asogbon MG, Geng Y, Jiang N, Mzurikwao D, Zheng Y et al (2021) Decoding movement intent patterns based on spatiotemporal and adaptive filtering method towards active motor training in stroke rehabilitation systems. Neural Comput Appl 33(10):4793–4806. https://doi.org/10.1007/s00521-020-05536-9
Santos EM, Cassani R, Falk TH, Fraga FJ (2020) Improved motor imagery brain-computer interface performance via adaptive modulation filtering and two-stage classification. Biomed Signal Process Control 57:101812. https://doi.org/10.1016/j.bspc.2019.101812
Sengupta A (2020) Study of cognitive fatigue using EEG entropy analysis. In: 2020 International conference on emerging frontiers in electrical and electronic technologies (ICEFEET), pp 1–6. https://doi.org/10.1109/ICEFEET49149.2020.9186989
Shepelev IE, Lazurenko DM, Kiroy VN, Aslanyan EV, Bakhtin OM, Minyaeva NR (2018) A novel neural network approach to creating a brain-computer interface based on the EEG patterns of voluntary muscle movements. Neurosci Behav Physiol 48(9):1145–1157. https://doi.org/10.1007/s11055-018-0679-0
Shcherban IV, Kirilenko NE, Shcherban OG (2018) Effective cost functions for spectrum entropy to search for high-frequency event-related patterns in electrograms with noise. Informatsionno-Upravliaiushchie Sistemy [information and Control Systems] 2:8–17. https://doi.org/10.15217/issn1684-8853.2018.2.8
Shcherban IV, Kirilenko NE, Krasnikov SO (2019) A search method for unknown high-frequency oscillators in noisy signals based on the continuous wavelet transform. Autom Remote Control 80(7):1279–1287. https://doi.org/10.1134/S0005117919070051
Shcherban IV, Kosenko PO, Shcherban OG, Lobzenko PV (2020) Method of automatic search for odor-induced patterns in bioelectric activity of a rat olfactory bulb. Inf Control Syst 5:62–69. https://doi.org/10.31799/1684-8853-2020-5-62-69
Shibasaki H, Hallett M (2006) What is the Bereitschaftspotential? Clin Neurophysiol 117(11):2341–2356. https://doi.org/10.1016/j.clinph.2006.04.025
Taha A, Hanbury A (2015) An efficient algorithm for calculating the exact Hausdorff distance. IEEE Trans Pattern Anal Mach Intell 37(11):2153–2163. https://doi.org/10.1109/TPAMI.2015.2408351
Takashima S, Ogawa CY, Najman FA, Ramos RT (2020) The volition, the mode of movement selection and the readiness potential. Exp Brain Res 238(10):2113–2123. https://doi.org/10.1007/s00221-020-05878-9
Taran S, Bajaj V (2019) Motor imagery tasks-based EEG signals classification using tunable-Q wavelet transform. Neural Comput Appl 31(11):6925–6932. https://doi.org/10.1007/s00521-018-3531-0
Türk Ö, Özerdem MS (2019) Epilepsy detection by using scalogram based convolutional neural network from EEG signals. Brain Sci 9(5):115. https://doi.org/10.3390/brainsci9050115
Vizilter YuV, Zheltov SYu (2014) Similarity measures and comparison metrics for image shapes. J Comput Syst Sci Int 53(4):542–555. https://doi.org/10.1134/S1064230714040169
Wang K, Xu M, Wang Y, Zhang S, Chen L, Ming D (2020) Enhance decoding of premovement EEG patterns for brain-computer interfaces. J Neural Eng 17(1):016033. https://doi.org/10.1016/j.neunet.2020.01.027
Walden A (2000) A unified view of multitaper multivariate spectral estimation. Biometrika 87(4):767–788. https://doi.org/10.1093/biomet/87.4.767
Xu S, Zhu L, Kong W, Peng Y, Hu H, Cao J (2021) A novel classification method for EEG-based motor imagery with narrow band spatial filters and deep convolutional neural network. Cogn Neurodynamics. https://doi.org/10.1007/s11571-021-09721-x
Zapała D, Zabielska-Mendyk E, Augustynowicz P, Cudo A, Jaśkiewicz M, Szewczyk M, Francuz P (2020) The effects of handedness on sensorimotor rhythm desynchronization and motor-imagery BCI control. Sci Rep 10(1):1–11. https://doi.org/10.1038/s41598-020-59222-w